Research Article | Vol. 8, No. 2 | 1 Feb 2017 | BIOMEDICAL OPTICS EXPRESS 524
Biomedical Optics EXPRESS

Clinical characterization of *in vivo* inflammatory bowel disease with Raman spectroscopy

Isaac J. Pence,[1] Dawn B. Beaulieu,[2] Sara N. Horst,[2] Xiaohong Bi,[3] Alan J. Herline,[2,4] David A. Schwartz,[2] and Anita Mahadevan-Jansen[1,*]

[1]*Department of Biomedical Engineering, Vanderbilt University, Nashville, Tennessee 37235, USA*
[2]*Division of Gastroenterology, Hepatology & Nutrition, Department of Medicine, Vanderbilt University Medical Center, Nashville, Tennessee 37235, USA*
[3]*Department of Nanomedicine and Biomedical Engineering, University of Texas Health Science Center at Houston, Houston, Texas 77054, USA*
[4]*Department of Surgery, Medical College of Georgia, Augusta, Georgia 30912, USA*
[*]*Anita.Mahadevan-Jansen@vanderbilt.edu*

Abstract: Inflammatory bowel disease (IBD), including ulcerative colitis (UC) and Crohn's disease (CD), affects over 1 million Americans and 2 million Europeans, and the incidence is increasing worldwide. While these diseases require unique medical care, the differentiation between UC and CD lacks a gold standard, and therefore relies on long term follow up, success or failure of existing treatment, and recurrence of the disease. Here, we present colonoscopy-coupled fiber optic probe-based Raman spectroscopy as a minimally-invasive diagnostic tool for IBD of the colon (UC and Crohn's colitis). This pilot *in vivo* study of subjects with existing IBD diagnoses of UC (n = 8), CD (n = 15), and normal control (n = 8) aimed to characterize spectral signatures of UC and CD. Samples were correlated with tissue pathology markers and endoscopic evaluation. The collected spectra were processed and analyzed using multivariate statistical techniques to identify spectral markers and discriminate IBD and disease classes. Confounding factors including the presence of active inflammation and the particular colon segment measured were investigated and integrated into the devised prediction algorithm, reaching 90% sensitivity and 75% specificity to CD from this *in vivo* data set. These results represent significant progress towards improved real-time classification for accurate and automated *in vivo* detection and discrimination of IBD during colonoscopy procedures.

OCIS codes: (170.5660) Raman spectroscopy; (170.3890) Medical optics instrumentation; (170.6935) Tissue characterization; (170.6510) Spectroscopy, tissue diagnostics;

References and links

1. A. N. Ananthakrishnan, "Epidemiology and risk factors for IBD," Nat. Rev. Gastroenterol. Hepatol. **12**(4), 205–217 (2015).
2. R. N. Baldassano and D. A. Piccoli, "Inflammatory bowel disease in pediatric and adolescent patients," Gastroenterol. Clin. North Am. **28**(2), 445–458 (1999).
3. R. S. Sandler, J. E. Everhart, M. Donowitz, E. Adams, K. Cronin, C. Goodman, E. Gemmen, S. Shah, A. Avdic, and R. Rubin, "The burden of selected digestive diseases in the United States," Gastroenterology **122**(5), 1500–1511 (2002).
4. C. Gunnarsson, J. Chen, J. A. Rizzo, J. A. Ladapo, and J. H. Lofland, "Direct Health Care Insurer And Out-of-Pocket Expenditures of inflammatory Bowel Disease: Evidence from a US National Survey," Dig. Dis. Sci. **57**(12), 3080–3091 (2012).
5. C. D. Stone, "The economic burden of inflammatory bowel disease: clear problem, unclear solution," Dig. Dis. Sci. **57**(12), 3042–3044 (2012).
6. A. K. Shergill, J. R. Lightdale, D. H. Bruining, R. D. Acosta, V. Chandrasekhara, K. V. Chathadi, G. A. Decker, D. S. Early, J. A. Evans, R. D. Fanelli, D. A. Fisher, L. Fonkalsrud, K. Foley, J. H. Hwang, T. L. Jue, M. A. Khashab, V. R. Muthusamy, S. F. Pasha, J. R. Saltzman, R. Sharaf, B. D. Cash, and J. M. DeWitt; American

#276220 http://dx.doi.org/10.1364/BOE.8.000524
Journal © 2017 Received 20 Sep 2016; revised 23 Nov 2016; accepted 24 Nov 2016; published 4 Jan 2017

Biomedical Optics EXPRESS

Society for Gastrointestinal Endoscopy Standards of Practice Committee, "The role of endoscopy in inflammatory bowel disease," Gastrointest. Endosc. **81**(5), 1101–1121 (2015).
7. A. Kornbluth and D. B. Sachar, Practice Parameters Committee of the American College of Gastroenterology, "Ulcerative Colitis Practice Guidelines in Adults: American College Of Gastroenterology, Practice Parameters Committee," Am. J. Gastroenterol. **105**(3), 501–524 (2010).
8. G. R. Lichtenstein, S. B. Hanauer, and W. J. Sandborn; Practice Parameters Committee of American College of Gastroenterology, "Management of Crohn's disease in adults," Am. J. Gastroenterol. **104**(2), 465–484 (2009).
9. D. C. Baumgart, "The diagnosis and treatment of Crohn's disease and ulcerative colitis," Dtsch. Arztebl. Int. **106**(8), 123–133 (2009).
10. M. L. Corman, *Colon and Rectal Surgery* (Lippincott, 1989).
11. G. T. Martland and N. A. Shepherd, "Indeterminate colitis: definition, diagnosis, implications and a plea for nosological sanity," Histopathology **50**(1), 83–96 (2007).
12. D. H. Bruining and E. V. Loftus, Jr., "Technology Insight: new techniques for imaging the gut in patients with IBD," Nat. Clin. Pract. Gastroenterol. Hepatol. **5**(3), 154–161 (2008).
13. B. A. MacKalski and C. N. Bernstein, "New diagnostic imaging tools for inflammatory bowel disease," Gut **55**(5), 733–741 (2006).
14. E. Rodriguez-Diaz, C. Atkinson, L. I. Jepeal, A. Berg, C. S. Huang, S. R. Cerda, M. J. O'Brien, I. J. Bigio, F. A. Farraye, and S. K. Singh, "Elastic scattering spectroscopy as an optical marker of inflammatory bowel disease activity and subtypes," Inflamm. Bowel Dis. **20**(6), 1029–1036 (2014).
15. B. Shen, G. Zuccaro, Jr., T. L. Gramlich, N. Gladkova, P. Trolli, M. Kareta, C. P. Delaney, J. T. Connor, B. A. Lashner, C. L. Bevins, F. Feldchtein, F. H. Remzi, M. L. Bambrick, and V. W. Fazio, "In vivo colonoscopic optical coherence tomography for transmural inflammation in inflammatory bowel disease," Clin. Gastroenterol. Hepatol. **2**(12), 1080–1087 (2004).
16. R. Sinha, "Recent advances in intestinal imaging," Indian J. Radiol. Imaging **21**(3), 170–175 (2011).
17. J. Addis, N. Mohammed, O. Rotimi, D. Magee, A. Jha, and V. Subramanian, "Raman spectroscopy of endoscopic colonic biopsies from patients with ulcerative colitis to identify mucosal inflammation and healing," Biomed. Opt. Express **7**(5), 2022–2035 (2016).
18. R. Malini, K. Venkatakrishna, J. Kurien, K. M. Pai, L. Rao, V. B. Kartha, and C. M. Krishna, "Discrimination of normal, inflammatory, premalignant, and malignant oral tissue: a Raman spectroscopy study," Biopolymers **81**(3), 179–193 (2006).
19. I. Pence and A. Mahadevan-Jansen, "Clinical instrumentation and applications of Raman spectroscopy," Chem. Soc. Rev. **45**(7), 1958–1979 (2016).
20. M. Agenant, M. Grimbergen, R. Draga, E. Marple, R. Bosch, and C. van Swol, "Clinical superficial Raman probe aimed for epithelial tumor detection: Phantom model results," Biomed. Opt. Express **5**(4), 1203–1216 (2014).
21. R. L. McCreery, *Raman Spectroscopy for Chemical Analysis* (New York: John Wiley & Sons, New York, 2000).
22. C. A. Lieber and A. Mahadevan-Jansen, "Automated method for subtraction of fluorescence from biological Raman spectra," Appl. Spectrosc. **57**(11), 1363–1367 (2003).
23. B. Krishnapuram, L. Carin, M. A. T. Figueiredo, and A. J. Hartemink, "Sparse multinomial logistic regression: fast algorithms and generalization bounds," IEEE Trans. Pattern Anal. Mach. Intell. **27**(6), 957–968 (2005).
24. I. J. Pence, C. A. Patil, C. A. Lieber, and A. Mahadevan-Jansen, "Discrimination of liver malignancies with 1064 nm dispersive Raman spectroscopy," Biomed. Opt. Express **6**(8), 2724–2737 (2015).
25. X. Bi, A. Walsh, A. Mahadevan-Jansen, and A. Herline, "Development of spectral markers for the discrimination of ulcerative colitis and Crohn's disease using Raman spectroscopy," Dis. Colon Rectum **54**(1), 48–53 (2011).
26. C. Bielecki, T. W. Bocklitz, M. Schmitt, C. Krafft, C. Marquardt, A. Gharbi, T. Knösel, A. Stallmach, and J. Popp, "Classification of inflammatory bowel diseases by means of Raman spectroscopic imaging of epithelium cells," J. Biomed. Opt. **17**(7), 0760301 (2012).
27. B. W. Barry, H. G. M. Edwards, and A. C. Williams, "Fourier-Transform Raman and Infrared Vibrational Study of Human Skin - Assignment of Spectral Bands," J. Raman Spectrosc. **23**(11), 641–645 (1992).
28. D. C. B. Redd, Z. C. Feng, K. T. Yue, and T. S. Gansler, "Raman-Spectroscopic Characterization of Human Breast Tissues - Implications for Breast-Cancer Diagnosis," Appl. Spectrosc. **47**(6), 787–791 (1993).
29. R. Manoharan, Y. Wang, and M. S. Feld, "Histochemical analysis of biological tissues using Raman spectroscopy," Spectrochimica Acta Part a-Molecular and Biomolecular Spectroscopy **52**(2), 215–249 (1996).
30. I. J. Pence, E. Vargis, and A. Mahadevan-Jansen, "Assessing variability of in vivo tissue Raman spectra," Appl. Spectrosc. **67**(7), 789–800 (2013).
31. M. S. Bergholt, W. Zheng, K. Lin, K. Y. Ho, M. Teh, K. G. Yeoh, J. B. Y. So, and Z. Huang, "Characterizing variability in in vivo Raman spectra of different anatomical locations in the upper gastrointestinal tract toward cancer detection," J. Biomed. Opt. **16**(3), 037003 (2011).
32. M. S. Bergholt, W. Zheng, K. Lin, J. Wang, H. Xu, J. L. Ren, K. Y. Ho, M. Teh, K. G. Yeoh, and Z. Huang, "Characterizing variability of in vivo Raman spectroscopic properties of different anatomical sites of normal colorectal tissue towards cancer diagnosis at colonoscopy," Anal. Chem. **87**(2), 960–966 (2015).
33. D. N. Granger, J. A. Barrowman, and P. R. Kvietys, *Clinical Gastrointestinal Physiology* (Saunders, 1985).
34. M. H. Ross and W. Pawlina, *Histology* (Lippincott Williams & Wilkins, 2006).
35. B. Young, *Wheater's Functional Histology: A Text and Colour Atlas* (Churchill Livingstone/Elsevier, Edinburgh, 2006).

Biomedical Optics EXPRESS

1. Introduction

Inflammatory bowel disease (IBD), which includes ulcerative colitis (UC) and Crohn's disease (CD), affects nearly one million Americans and two million Europeans, and the incidence is increasing worldwide [1]. This complex illness is characterized by both chronic and acute disease states, with periods of inflammatory flare, quiescence, and relapse. Ulcerative colitis is almost always confined to the colon and Crohn's disease may occur in any part of the gastrointestinal tract from the mouth to the rectum. Numerous overlapping risk factors including ethnic origin, lifestyle, geographic region, and susceptibility regions on at least 12 chromosomes confound physiological understanding of this disease [2, 3]. Patients with IBD have an elevated risk of gastrointestinal cancer and experience dramatic decreases in quality of life. Despite advances in therapy, hospitalization rates for IBD, particularly CD, have shown significant increase, incurring a substantial rise in inflation-adjusted economic burden. With the high drug costs and rates of surgery (up to 75% of CD and 25-33% of UC patients), IBD is one of the costliest conditions on a per year basis in the US, with expenses for CD surpassing diabetes, coronary artery disease, and chronic obstructive pulmonary disease [4, 5].

Despite the overlap in presentation, symptoms, and progression of CD and UC, discriminating IBD subtype is vital for selection of the most appropriate therapeutic or surgical intervention and patient prognosis, a determination often made by assessing the severity of active inflammation during evaluation. For instance, UC can be cured in many patients by surgical removal of the colon, however, CD surgeries are rarely curative and often require further procedures. The goal of IBD treatment is to rapidly induce remission and prevent disease complications. Currently, the distinction between UC and CD is made based on inexact clinical, radiologic, endoscopic, and pathologic features [6–9]; in up to 15% of IBD cases indeterminate colitis (IC, or IBD unspecified) is diagnosed because of the difficulty in distinguishing between UC and CD. In these patients, diagnosis ultimately relies on long term follow up based on success or failure of existing treatment and recurrence of disease. A further challenge is that another 5-14% of cases are reclassified within IBD based on long-term follow up [10, 11]. All of these determinations are complicated by the lack of a definitive, recognized gold standard for diagnosis. Therefore, accurate differential diagnosis of IBD is critically needed for appropriate medical and surgical care, intervention, and prognosis. The development of new technologies that can improve understanding of IBD and aid objective diagnosis may help meet this need.

Clinically, diagnosis is made primarily based upon symptom presentation (abdominal pain, number and consistency of stools, etc) and biopsy informed video endoscopy (White Light Reflectance, WLR). While the disease may manifest in a typical and easily characterized fashion in some patients, expert endoscopists often face non-differentiating disease appearance and histopathologists can only identify features of chronic or acute colon inflammation that are consistent with both IBD subtypes. The lack of a definitive, biochemically specific characterization tool that can investigate IBD subtypes directly hinders delivery of appropriate care. Numerous investigations have been pursued to develop tools to improve diagnosis, including computed tomography, magnetic resonance imaging, optical coherence tomography, laser endomicroscopy, wireless capsule endoscopy, and elastic scattering spectroscopy [12–16]. All of these techniques are based on structure either at the macroscopic (appearance under widefield imaging) or microscopic scale (cell morphology and optical scattering properties of tissues). However, structural changes in tissue are a downstream effect of underlying disease presentation and have not proven effective for IBD differentiation. Raman scattering, on the other hand, is sensitive to the constituent biomolecular makeup of a sample, and can be utilized to capture a fingerprint of the vibrational modes of chemical bonds present within tissue. It is expected that unique biochemical alterations associated with inflammatory response pathways will precede macroscopic tissue changes [17, 18]. These disease specific changes in tissues that are

Biomedical Optics EXPRESS

associated with disease status, on both the macro- and microscopic scales should provide valuable information to differentiate IBD in the colon.

Raman spectroscopic techniques have been investigated for numerous clinical diagnostic applications to aid in real-time objective disease evaluation [19]. Specifically addressing IBD, Raman techniques have been applied for *ex vivo* tissues to develop preliminary biomarkers and identify spectral signatures consistent with disease subtype. The goal of this study is to demonstrate the potential for Raman spectroscopy to detect tissue changes consistent with inflammatory bowel disease in the colon as a potential diagnostic adjunct. This report presents results from an endoscopic study using Raman spectroscopy to characterize IBD from human subjects *in vivo*. This work characterizes the disease presentation from a diverse patient population and demonstrates disease discrimination based on spectral changes measured across subjects *in vivo*. Furthermore, this work sought to elucidate confounding factors that limit predictive performance and incorporate these factors to improve rates of disease classification. Overall, results demonstrate the potential for endoscopic Raman spectroscopy as a diagnostic adjunct for IBD.

2. Methods

Subject recruitment and measurement protocol

Following written informed consent, 23 patients with IBD diagnoses (Table 1) that were scheduled for a routine surveillance and evaluation colonoscopy at the Vanderbilt GI Endoscopy lab were recruited according to IRB protocol (IRB #111609). Furthermore, healthy control subjects with no history of inflammatory disease were recruited from the population of colon cancer screening patients at the endoscopy lab. Following standard colonoscopy protocol but prior to biopsy as indicated, spectra were obtained from normal and/or inflamed sites within the colon, making measurements at two distinct sites in each segment: right (cecum or ascending), transverse, and left (descending or sigmoid) colon, as well as two sites in the rectum. The surface of the colon at each measurement site was flushed with saline to clear mucus, blood, or debris prior to spectral acquisition. The probe was introduced through the endoscope accessory channel once the measurement location was reached. With the probe touching the mucosal surface with sufficient pressure to ensure gentle contact while maintaining position during each measurement, spectra were collected and averaged per site while the endoscope's white light was disabled. The probed site was then biopsied and the tissue samples were fixed in formalin for routine histopathology. Spectra were compared with the combined physician evaluation based on endoscopy, histopathology, and patient history (consistent with standard of care) for the respective gold standard patient diagnosis. Between subjects, the probe was detached from the system for cleaning, soaked in ortho-Phthalaldehyde (Cidex OPA, Johnson & Johnson, Arlington, TX) and rinsed thoroughly with water, in accordance with clinical protocols for high-level disinfection.

Table 1. Description of study participants

Normal control (NC)	**n = 8**
Age (years)	56.6 ± 9.3
BMI	31.3 ± 6.9
Gender	6F, 2M
Crohn's disease (CD)	**n = 15**
Age	39.7 ± 7.6
BMI	26.1 ± 4.3
Gender	12F, 3M
Ulcerative colitis (UC)	**n = 8**
Age	44.8 ± 12.2
BMI	27.0 ± 5.8
Gender	3F, 5M

Biomedical Optics EXPRESS

Raman instrumentation, calibration and processing

In vivo Raman spectra were collected using a portable clinical Raman spectroscopy system coupled to a standard clinical endoscope (Fig. 1). A 785 nm diode laser (Innovative Photonics Solutions, Monmouth Junction, NJ) was coupled to a custom-fabricated superficially focused fiber-optic probe (EmVision LLC, Loxahatchee, FL) which delivered 80 mW to the surface of the colon. Briefly, the endoscope compatible fiber optic probe contains a 200 μm core diameter excitation fiber with bandpass filtering surrounded by seven 300 μm collection fibers with long pass filters. A shallow focusing micro lens composed of a plano-convex sapphire lens and MgF_2 optical window is placed in front of the filters to maximize collection efficiency at the probe tip [20]. The probe tip is physically packaged in a 2.1 mm diameter rigid metal tube that is approximately 6 mm in length to couple with standard endoscope technology. Each measurement utilized three integrated spectra of 250 ms acquisitions to achieve a sufficient signal to noise ratio (SNR ≥15) [21]. Longer integration times could not be utilized due to the substantial background and autofluorescence signals generated by the tissue. The Raman scattered light was collected in reflectance mode and coupled into an f/1.8 spectrograph (Kaiser Optical Systems, Inc.) with a fixed volume phase holographic grating resulting in spectral coverage from 450 to 1950 cm^{-1} and a spectral resolution of 7 cm^{-1}. The detector was a back-illuminated deep-depletion CCD which was thermoelectrically cooled to −70°C (Pixis 256BR, Princeton Instruments). Spectral calibration was performed using a neon–argon lamp with naphthalene and acetaminophen standards to correct for day-to-day variations. A National Institute of Standards and Technology-certified quartz-tungsten halogen lamp was used to account for the wavelength-dependent response of the instrument. The spectra were processed for fluorescence subtraction and noise smoothing using the modified polynomial fit and Savitzky–Golay methods, and subsequently normalized to the spectrum mean as described previously [22]. All calibration steps were performed in the procedure room prior to the beginning of each case, and post-processing steps were completed within 1-2 seconds after each measurement. The collection parameters were optimized during the first two procedures based upon sensitivity of the probe design and system. Statistical differences for integrated spectral intensity and colons segment were performed independently using ANOVA with $\alpha = 0.05$.

Biomedical Optics EXPRESS

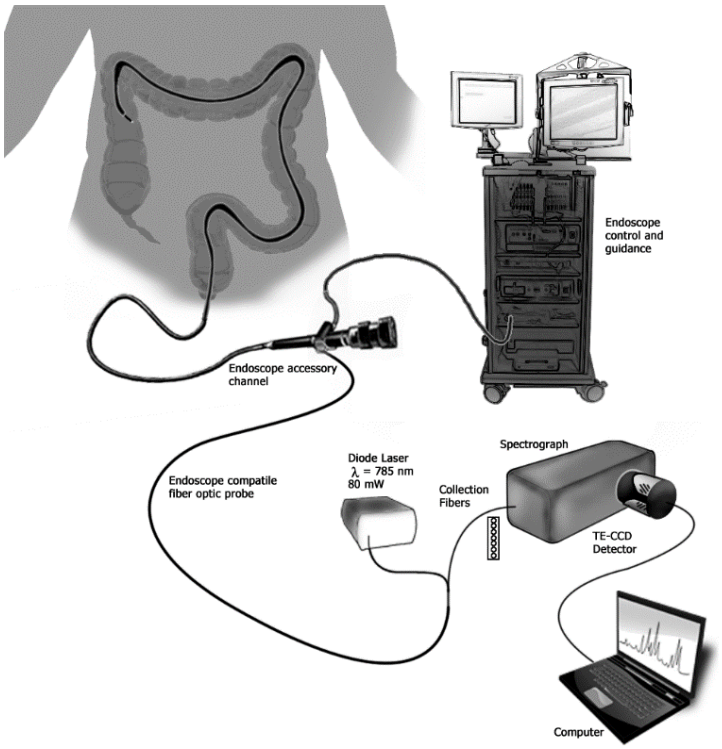

Fig. 1. Schematic of integrated Raman and endoscope instrumentation for *in vivo* subject measurement. Components are not drawn to scale.

Classification algorithm: sparse multinomial logistic regression

The resulting spectra were classified with a Bayesian machine learning algorithm, sparse multinomial logistic regression (SMLR), to quantitatively determine the potential for Raman spectra to separate healthy and diseased colon tissues. SMLR is a versatile multiclass iterative algorithm that reduces the high dimensionality of Raman data to only those spectral basis features needed for discrimination [23, 24]. SMLR reduces the data set by creating a transformation of the original data in which distinguishing spectral basis features were weighted based on their ability to successfully separate classes of training data. The training and classification procedure implemented here used a Laplacian prior, a direct kernel, no bias, z-scored spectral normalization, component–wise updates, and leave-one-subject-out cross validation. A posterior probability of membership in each class was then calculated for each individual spectrum using a classifier trained only with spectra from other subjects. The final sensitivity and specificity for each classification test is reported either in relation to detecting disease (control versus IBD), or for differential discrimination (CD versus UC), to detecting Crohn's disease. Stratified classification based on variable disease presentation is achieved through using the appropriate subset of data prior to model training and cross validation.

3. Results

A comparison between mean spectra obtained from subjects within each disease category is depicted in Fig. 2. All signatures comprised lipid-rich features, with strong, narrow bands at 1300 cm^{-1}, 1440 cm^{-1}, and 1658 cm^{-1}. These average signals exhibit subtle interclass variations that indicate separation across the Raman fingerprint region (450-1800 cm^{-1}). Multivariate analysis techniques can be employed for pattern recognition and feature selection to take advantage of the feature rich signals for Raman spectra and IBD [24–26]. Fig. 3 depicts the performance of SMLR, where the separation of spectra measured from normal

Biomedical Optics EXPRESS

control subjects and from those with IBD is displayed for leave-one-subject-out cross validation along with several of the salient spectral features utilized for discrimination. The SMLR algorithm selects peaks and shoulders that significantly contribute to discrimination and is not limited to only prominent features. Tentative peak assignments for these discriminating features include 425 cm^{-1} (δ (CCC) skeletal backbone), 610 cm^{-1} (ρ(CH) wagging in proteins), 1080 cm^{-1} (ν(C–C) of lipids), 1440 cm^{-1} shoulder (δ(CH2) deformation of proteins and lipids), 1160 cm^{-1} and 1525 cm^{-1} (β-carotene), and 1741 cm^{-1} (ν(C = O) in lipids) [27, 28].

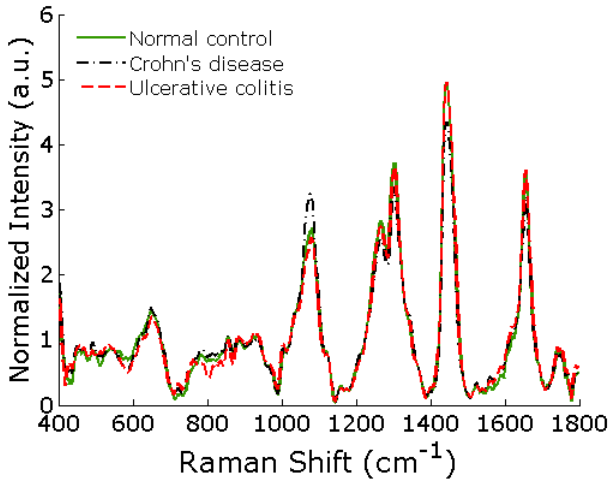

Fig. 2. Normalized mean *in vivo* Raman spectra obtained from subjects within each disease class.

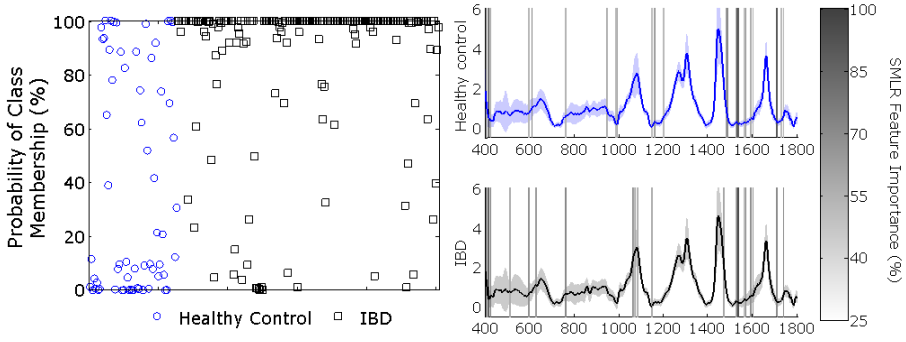

Fig. 3. (Left) Prediction performance describing the probability of group membership for *in vivo* spectra obtained from normal control and IBD subjects. (Right) Mean ± standard deviation spectra and 26 features utilized for discrimination are depicted.

This *in vivo* data set spans a diverse population of subjects and disease presentations; as such, multiple discrimination comparisons were of interest for this data set as indicated in the first column of Table 2. Independent training and cross validation sets were conducted to gauge unbiased classification performance for each comparison of interest. Table 2 comprises the results for several of these analyses including discrimination between disease and control as well as differential discrimination of IBD subtype. In general, test sensitivity was high when discriminating IBD from normal controls, but specificity was poor, achieving 86% and 39%, respectively. When discriminating spectra from control subjects and spectra measured from IBD subjects with active inflammation (determined during WLR endoscopy), specificity

Biomedical Optics EXPRESS

increased to 57%. For comparisons of normal control and inactive disease, specificity was lower, indicating that active inflammation is a factor that requires further attention. In discriminating between IBD subtypes, substantial differences in performance occur when considering subjects with active inflammation (83% sensitivity and 55% specificity) compared with quiescent disease (62% sensitivity and 22% specificity). Subsequent analysis addresses the impact of potential confounding factors through data stratification to evaluate classification performance.

Table 2. Classification performance for *in vivo* comparisons.

Comparison	Sensitivity (%)	Specificity (%)
Control v. IBD	86.2	39.7
Control v. Inactive IBD	81.1	44.4
Control v. Active IBD	78	57.1
Inactive IBD v. Active IBD	67.1	74.5
Inactive CD v. Inactive UC	62	22.9
Active CD v. Active UC	83.3	55.9

As demonstrated by the results comprising Table 2, the impact of active inflammation requires investigation and can be readily visualized in Fig. 4. In spectra measured from normal and quiescent IBD subjects (all inactive), mean spectral lineshapes exhibit strong and narrow lipid features and vary consistently across the majority of the fingerprint range regardless of disease class. By comparison, the mean spectra from actively inflamed colon segments are broader and less intense, resembling protein-based signatures rather than those of lipids. Furthermore, as visualized in Fig. 4 (right), there is a statistically significant decrease in spectral intensity as active inflammation occurs, and a decreasing trend as inflammation progresses in severity. These changes in spectral response due to severity of inflammation indicates a need to account for this factor in the discrimination algorithm. However, for all of the analyses presented in Table 2 disease subtype (CD and UC) and/or levels of inflammation activity (inactive – severe) were combined. Likewise, these comparisons did not address the impact caused by the segment of the colon from which the spectrum was acquired. Figure 5 depicts the mean and standard deviation of spectral variations present when *in vivo* measurements from normal control subjects are isolated to particular segments of the colon. Several prominent and subtle features differ in intensity between colon segment spectra: potential band assignments include 873 cm^{-1} ($\rho(CH_2)$ in proteins), 1160 cm^{-1} (β-carotene), 1265 cm^{-1} (ν(C-N) of Amide III), 1300 cm^{-1} (δ(CH2) deformation of proteins and lipids), 1372 cm^{-1} (lipid), and 1658 cm^{-1} (ν(C = O), Amide I and lipids) [18, 27–29]. These differences indicate the potential influence of colon segment on measured spectra and may impact to classification performance.

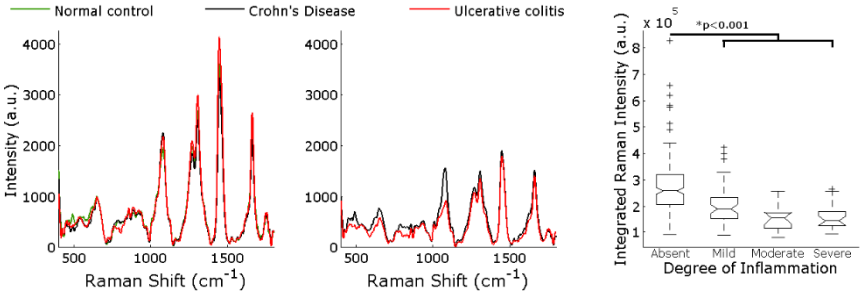

Fig. 4. Impact of active inflammation: Mean Raman spectra from all disease classes when no activity is present (left) and from IBD subtypes when active disease is present (center). Integrated Raman spectra for all data by level of activity (right) indicates significant differences between disease presentation and the potential for the development of an objective metric to characterize inflammatory disease activity.

Biomedical Optics EXPRESS

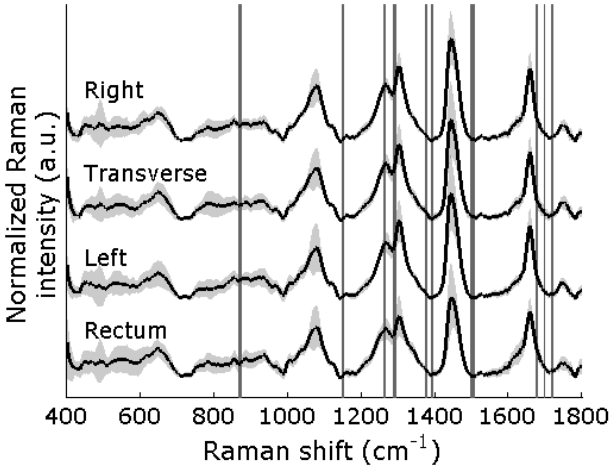

Fig. 5. Mean spectra from colon segments obtained from normal control subjects. Shaded regions along spectra indicate standard deviations. Variations can be seen across the spectral lineshapes between segment and significant features have been identified as a function of wavenumber (vertical gray bands).

Stratified classifiers were implemented by appropriately selecting spectra from a subset of the recruitment population in order to control for factors of disease location and severity. Based on the spectral changes imparted by both colon segment measured and the presence of active inflammation, these factors were incorporated into stratified classifiers, each resulting in a different number of patients (n, Table 3) that were considered for the evaluation. Table 3 comprises the results of leave-one-subject-out cross validation for 2-class IBD discrimination. The stratified classifier improves sensitivity and specificity compared with the prior performance for differentiating CD and UC when location and disease presentation are averaged (Table 2, Active CD versus Active UC). Once the measurement location and the severity of disease are incorporated, sensitivity to CD increases, for example from 83% to 90% and specificity from 56% to 75% in the right colon. While the performance varies between colon segments, in general, inclusion of inflammation and location factors caused an increase in a combination of sensitivity and specificity for spectra acquired during colonoscopy. These results support further investigation of influential variables for IBD discrimination, yet demonstrate the potential to improve classification accuracy for these complex, heterogeneous diseases.

Table 3. Classification performance for *in vivo* spectra from subjects with active IBD stratified by colon segment

Colon Segment	Sensitivity (to CD) %	Specificity (to CD) %
Right (n = 9)	90	75
Transverse (n = 5)	75	67
Left (n = 12)	85	45
Rectum (n = 11)	71	56

4. Discussion

Here, we report our recently developed endoscopy-coupled Raman spectroscopy technique that enables real-time measurements of tissue biomolecular constituents for *in vivo* differentiation and characterization of IBD in the colon. Prior work has demonstrated that Raman spectroscopy is sensitive to IBD subtype specific signatures in *ex vivo* tissue sample evaluations. In this work, we have applied this technique to probe the specific biochemical composition of the colon in real-time to provide an objective characterization of the colon

Biomedical Optics EXPRESS

tissue and disease status, discerning more information which could serve as a valuable adjunct for differential diagnosis of UC and CD and minimize the need for random sample biopsy protocols. While classic clinical parameters associated with a diagnosis of CD (lack of rectal disease, patchy colitis, and the presence of granulomas (found unusually) in histology) may all be indicators of a CD diagnosis, currently there is in general no universal feature that serves as a gold standard for differential diagnosis for IBD. As such, the results of this study were evaluated relative to the established diagnoses for the recruited patients that were made based upon patient history, clinical presentation, therapeutic response, histopathologic findings, and video endoscopy findings. The Vanderbilt Inflammatory Bowel Disease Center is a regional referral center, with extensive expertise following over 1,000 patients annually. For this study, no patients exhibiting IBD unspecified presentation were included in the analysis. These patients with indeterminate colitis are of particular interest as they could most benefit from new tools for disease differentiation.

Our endoscopy compatible Raman spectroscopy system has enabled rapid *in vivo* biochemically specific measurements from a diverse patient population with representative disease presentations (Table 1). The fiber optic probe design utilized herein enabled rapid, high SNR (≥15) contact measurements of the colon constituent biochemistry (Fig. 2) and coupled with standard endoscope accessory channel (Fig. 1). Prior work has demonstrated that excess pressure can alter spectral signatures, and thus attempts were made to minimize this factor [30]. Preliminary distinction of the study sample based on disease diagnosis generally indicates high sensitivity and low specificity, with a wide margin of performance depending upon the classification target (Table 2). When considering all study subjects together without controlling for disease presentation or subtype, discriminating disease from control has 86% sensitivity but only 39% specificity. This low specificity is further demonstrated in Fig. 3 (left), where a majority of spectra from IBD patients are correctly classified but few spectra from control subjects were correct. This classification was based on the selection of 26 features from the Raman spectrum, however in a separate classification step using a higher sparsity promoting factor yielded identical performance based on only 13 features. In considering the differential discrimination tests, sensitivity and specificity to Crohn's disease is drastically lower for quiescent (inactive) disease (62% and 22%, respectively; Table 2) compared with spectra acquired from patients with active disease (83% sensitivity and 55% specificity). These variations in prediction performance based on different classification targets reinforce the impact of disease variables on the acquired spectra and the need to properly control for disease variables.

The distinction between spectra from control subjects and those with quiescent disease in Table 2 (81% sensitivity, 41% specificity) indicates that colitis imparts a detectible change even when no active inflammation is present, a finding supported by changes to the vascular appearance of the tissue noted during WLR endoscopy [6]. When separating controls from IBD, combining spectra from subjects with and without active disease causes significant blurring of spectral distinct lineshapes (Fig. 4) and confounds the classifier. This result prompted further investigation of the influential sources of variance within the data set that, if accounted for, may allow improved performance. Active disease in the colon presents in a gradient of severity that has been discretized by the endoscopists in this study. However, when considering signals measured from subjects without active disease (including the normal control population), spectra are significantly stronger and exhibit intense lipid features (Fig. 4). However, when considering only spectra from active locations from IBD subjects, regardless of disease, the spectra are much weaker, and exhibit peak broadening consistent with increased protein content, potentially from fibrin and collagen and consistent with ulceration and edema [14, 17]. While these features themselves do not provide discrimination between CD and UC, there remains the potential that an objective metric for disease activity could be developed; such a metric could be used to evaluate therapeutic response after

Biomedical Optics EXPRESS

initiation of medication, for which a relative measure of active inflammation over time could be critical.

The differences in tissue for both disease presentation and healthy colon, which is functionally and biologically varied, require a thorough evaluation of inter-anatomical sites in order to characterize the impact on performance for disease separation. Based on the low sensitivity displayed for several tests in Table 2, including differential discrimination of active CD and UC, we hypothesized that other factors were confounding disease prediction. This *in vivo* study represents a pilot evaluation of some of these native factors that cannot be investigated with *ex vivo* tissue sections and indicates the potential for *in vivo* characterization and discrimination. Studies by other groups investigating *ex vivo* discrimination of IBD or the influence of colon segment and disease activity have produced outcomes that support our findings and may lead to an improved understanding of the factors that belie the detected spectral differences [17, 25, 26]. While the report of spectral differences between anatomical sites (Fig. 5) is corroborated by other investigations in the stomach and colon [31, 32], the exact cause of the spectral changes is thus far uncertain. Potential differences include bowel thickness and mucosal morphology, vascular density, proximity to mesentery, gland content and microbe distribution, among others [33–35]. The complexity of these *in vivo* measurements, impacted by both biomolecular and morphological changes in the tissue, require further characterization that is beyond the scope of this study. However, classification performance improved when colon segment was integrated into the algorithm, further supporting the need of improved characterization.

Disease severity and colon segment are only a few of the potential influences on the performance for IBD evaluation and discrimination based on *in vivo* Raman spectra. Other factors not yet considered based on subject recruitment for this pilot study include gender, age, BMI, diet, and prior therapeutic treatments, among others. While such factors likely impact classification, incorporation of both colon segment and disease severity factors into the IBD discrimination algorithm achieved increases to 90% sensitivity and 75% specificity to IBD subtype in the right colon (Table 3). The variation in prediction performance appears to be linked to the relative distribution of IBD subtypes for patients included in the classification but with expanded recruitment, these values will approach the true prediction rate. These results demonstrate that by properly assessing disease related variables and including them in the analysis, prediction performance can be improved for *in vivo* Raman spectroscopy applications. This also implies the need for *a priori* knowledge for inclusion in distinct classifiers; however, colon segment and disease activity can be determined during video endoscopy in real-time. Furthermore, the duration of data acquisition, processing, and prediction are short enough that such information could be incorporated into the real-time interface providing immediate feedback to the clinicians during routine evaluations. The results of this work demonstrate the potential for *in vivo* Raman spectroscopy to impact IBD evaluation and the prospect for staging and discrimination. Continued development of this sensitive technique could also provide new information to better understand and categorize disease for patients with indeterminate colitis diagnoses.

In summary, this study indicates that *in vivo* Raman spectra for IBD can be acquired non-destructively and in real-time in human subjects from the colon during routine surveillance endoscopy with high SNR. The resultant spectra have a wealth of information content that can discriminate between IBD and normal colon, as well as indicate the level of disease activity present. Furthermore, preliminary investigation of influential factors for discrimination indicate that disease severity and colon segment measured should be accounted for during evaluation. In combination with standard endoscopic evaluation, Raman spectroscopy has the potential for providing previously unobtainable biochemical information that may be useful as a diagnostic adjunct for IBD.

Biomedical Optics EXPRESS

Funding

We would like to acknowledge funding support from American Society for Lasers in Medicine and Surgery student research grant and National Institutes of Health NRSA F31 predoctoral fellowship.

Acknowledgments

The authors would like to acknowledge Dr. Quyen Nguyen for invaluable discussion as well as the staff of the Vanderbilt GI Endoscopy lab that helped facilitate patient recruitment and measurement.